Spin and orbital ordering in double-layered manganites

Ryo Maezono and Naoto Nagaosa
Department of Applied Physics, University of Tokyo, Bunkyo-ku, Tokyo 113-8656, Japan
(Received 23 April 1999)

We study theoretically the phase diagram of the double-layered perovskite manganites taking into account the orbital degeneracy, the strong Coulombic repulsion, and the coupling with the lattice deformation. Observed spin structural changes such as increased doping, are explained in terms of the orbital ordering and the bond-length dependence of the hopping integral along the *c* axis. Temperature dependence of the neutron diffraction peak corresponding to the canting structure is also explained. Comparison with the three-dimensional cubic system is made.

I. INTRODUCTION

Perovskite manganites $(R_{1-x},A_x)_{n+1}Mn_nO_{3n+1}$ (R=La, Pr, Nd, Sm; A=Ca, Sr, Ba; $n=1,2,\infty$) have recently attracted renewed interests from the viewpoint of the close connection between magnetism and transport.[1–6] The stability of the perovskite structure enables the preparation of high-quality single crystals with systematically changing the carrier density and the bandwidth by controlling R and A atoms. In addition, the crystal structure changes from two-dimensional ($n=1$, single layer) to three-dimensional ($n=\infty$, cubic) as n increases. The dimensionality of the electronic structure is controlled also by the spin and the orbital orderings, for example, the transfer along *c* axis is forbidden by the antiparallel spin configuration and/or the $d_{x^2-y^2}$ orbital ordering.[7,8] Therefore even in the isotropic ($n=\infty$, cubic, 113 system) crystal structure, the electronic dispersion can be quasi-two-dimensional [layered antiferromagnetic (spin A) in $Pr_{1-x}Sr_xMnO_3$,[9,10] $Nd_{1-x}Sr_xMnO_3$,[11–13] $La_{1-x}Sr_xMnO_3$ (Ref. 14)] or quasi-one-dimensional [rod type AF (spin C) in $Nd_{1-x}Sr_xMnO_3$ (Refs. 11 and 12)]. Another important related issue is the spin canting. As discussed by de Gennes,[15] A-type antiferromagnet near the parent insulator is unstable toward the spin canting when holes are doped. This is because the kinetic energy gain along *c* axis wins the energy cost of the AF exchange interaction for small canting angle. In the metallic A-type AF phase mentioned above, however, no spin canting has been observed.[9]

Double-layered manganites with $n=2$ (327 system) offer an interesting opportunity to study the interplay of the spin, the orbital and the crystal structure in the above-mentioned issues of dimensionality and spin canting. With increasing x, the spin ordering within one double layer changes from the ferromagnetic one (spin F, $x=0.3$) to the spin A ($x=0.5$).[6,16–26] For $0.4<x<0.48$ the diffraction peak observed in the neutron-scattering experiments indicates the coexistance of the spin F and A components at low temperatures, which has been interpreted as the spin canting.[19–22,25,26] However it could be interpreted also in terms of the phase separation, and further theoretical studies are needed. Lattice deformation depending upon x is also observed,[18,22–26] implying active contribution to the spin transition, in comparison with 113 system. In 113 system, there is the one-to-one correspondence between the crystal deformation and the orbital ordering, e.g., the *c* axis contracts in the metallic spin A state[13] where the $d_{x^2-y^2}$ ordering occurs.[8] In 327 system, on the other hand, MnO_6 octahedra elongate along *c* axis during the spin structural change from spin F to cant, and to spin A.[24] This elongation decreases with increasing x up to $x=0.5$ continuously, but even in the spin A phase a little elongation remains,[24] though this deformation prefers the $d_{3z^2-r^2}$.

In this paper, we study the spin and the orbital ordering in the double-layered compounds. Possibility of the spin canting is studied for general x, which includes the de Gennes's canting mechanism as a special case. In the metallic region, the spin A is locally stable against the spin canting. Spin transition from the spin A is therefore discontinuous one to the spin canting or to the spin F, depending on the ratio of the transfer integral and the superexchange interaction between t_{2g} spins. For the spin canting to occur in the metallic region, the small transfer integral along *c* axis, i.e., the planar orbital ordering, turned out to be indispensable. The canting angle is sensitive to the bond length along *c* axis. With this mechanism, calculated mean-field phase diagram together with the observed lattice distortion[18,22–25] can qualitatively explain the observed x (Refs. 6,16–26) and T dependence[22] of the spin ordering and also the spin anisotropy[20,22,26,27] in 327 system.

The plan of this paper follows. In Sec. II, the model and the formulation are given. Results and discussion are presented in Sec. III. Notations used here are standard as in Ref. 8.

II. MODEL AND FORMULATION

We start with the Hamiltonian

$$H=\sum_{\sigma\gamma\gamma'\langle ij\rangle} t_{ij}^{\gamma\gamma'} d_{i\sigma\gamma}^{\dagger} d_{j\sigma\gamma'} - J_H \sum_i \vec{S}_{t_{2g}i}\cdot\vec{S}_{e_g i} + J_S \sum_{\langle ij\rangle} \vec{S}_{t_{2g}i}\cdot\vec{S}_{t_{2g}j} + H_{\text{on site}} + H_{\text{el-ph}}, \quad (1)$$

where γ [$=a(d_{x^2-y^2}),b(d_{3z^2-r^2})$] specifies the orbital and the other notations are standard. The transfer integral $t_{ij}^{\gamma\gamma'}$ depends on the pair of orbitals (γ,γ') and the direction of the bond (i,j)[28], J_H is the Hund coupling between e_g and t_{2g}

spins, and J_S is the AF coupling between nearest neighboring t_{2g} spins. $H_{\text{on site}}$ represents the on-site Coulomb interactions between e_g electrons, and is given by[8,28]

$$H_{\text{on site}} = -\sum_i (\tilde{\beta}\vec{T}_i^{\,2} + \tilde{\alpha}\vec{S}_{e_g i}^{\,2}), \tag{2}$$

where the spin operator for the e_g electron is defined as $\vec{S}_{e_g i} = \frac{1}{2}\Sigma_{\gamma\alpha\beta} d_{i\gamma\alpha}^{\dagger} \vec{\sigma}_{\alpha\beta} d_{i\gamma\beta}$ with the Pauli matrices $\vec{\sigma}$, while the orbital isospin operator is defined as $\vec{T}_i = \frac{1}{2}\Sigma_{\gamma\gamma'\sigma} d_{i\gamma\sigma}^{\dagger} \vec{\sigma}_{\gamma\gamma'} d_{i\gamma'\sigma}$. Coefficients of the spin and isospin operators, i.e., $\tilde{\alpha}$ and $\tilde{\beta}$, are given by[8,28] $\tilde{\alpha} = U - J/2 > 0$, and $\tilde{\beta} = U - 3J/2 > 0$. The minus sign in Eq. (2) means that the Coulomb interactions induce both spin and orbital (isospin) moments. The parameters $\tilde{\alpha}, \tilde{\beta}, t_0$, used in the numerical calculation are chosen as $t_0 = 0.72$ eV, $U = 6.3$ eV, and $J = 1.0$ eV, being relevant to the actual manganese oxides.[7,8] The electron-lattice interaction is[8]

$$H_{\text{el-ph}} = +|g| r \sum_i \vec{v}_i \cdot \vec{T}_i, \tag{3}$$

where g is the coupling constant and r ($\vec{v}_i$) is the magnitude (direction) of the lattice distortion of the MnO_6 octahedra. Values of r and $\vec{v}$ are taken from the observed elongation along c axis in $(La_{1-x}, Sr_x)_3Mn_2O_7$ ($0.3 < x < 0.4$) (Ref. 24) leading to $r \sim 0.01$, $\vec{v} // \hat{z}$. We calculate the ground state energy by the mean-field approximation with the two order parameters,[8]

$$\vec{\varphi}_S = \langle \vec{S}_{e_g} \rangle + \frac{J_H}{2\tilde{\alpha}} \langle \vec{S}_{t_{2g}} \rangle, \tag{4}$$

$$\vec{\varphi}_T = \langle \vec{T} \rangle. \tag{5}$$

As the exchange interaction between two double layers is reported to be less than 1/100 compared with the intra double-layer one,[29] we consider an isolated double layer, for which the Brillouin zone contains only two $\vec{k}$ points along c axis. We consider four kinds of the spin alignment in the cubic cell: spin F, A, C, and G (NaCl type). For spin A, we also consider the possibility of the canting characterized by an angle η which is 0 (π) for spin F (A). As for the orbital degrees of freedom, we consider two sublattices I, and II, on each of which the orbital is specified by the angle $\theta_{I,II}$ as[8]

$$|\theta_{I,II}\rangle = \cos\frac{\theta_{I,II}}{2} |d_{x^2-y^2}\rangle + \sin\frac{\theta_{I,II}}{2} |d_{3z^2-r^2}\rangle. \tag{6}$$

We also consider four types of orbital-sublattice ordering, i.e., F-, A-, C-, G-type in the cubic cell. Henceforth, we often use a notation such as spin A, orbital G (θ_I, θ_{II}), etc. Denoting the wave vector of the spin (orbital) ordering as $\vec{q}_S$ ($\vec{q}_T$), the ground-state energy is given as a function of the spin ordering (η, $\vec{q}_S$), the orbital ordering ($\theta_{I,II}$, $\vec{q}_T$), and the lattice distortion (g, r, $\vec{v}$).

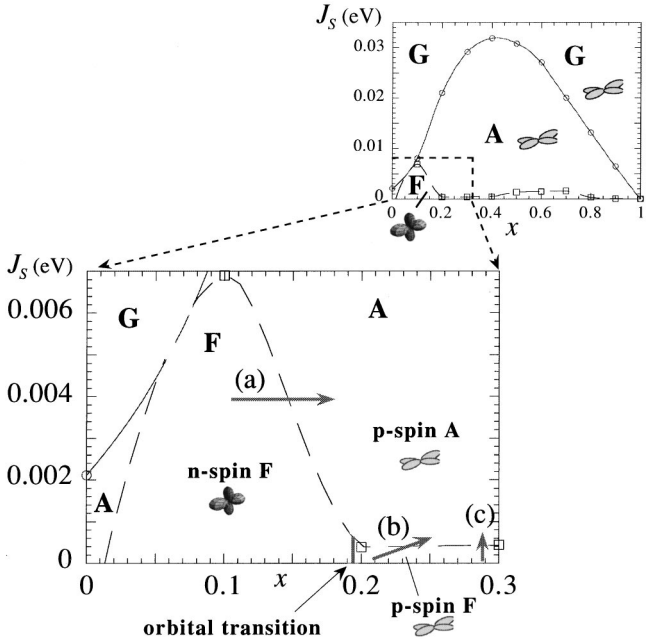

FIG. 1. Phase diagram at zero temperature in the plane of the doping concentration (x) and the AF interaction between t_{2g} spins (J_S), without electron-lattice coupling ($g = 0$). Orbital shape is represented by p- [planar, orbital F (0,0), i.e., $d_{x^2-y^2}$] and n-[not planar, orbital G (100,−100) around $x = 0.1$ and orbital A (−40,−40) around $x = 0.7$]. The possibility of the spin canting is not taken into account ($\eta = 0, \pi$). Depicted arrow (a) [(b)] corresponds to the spin transition with fixed (increasing) J_S.

III. RESULTS AND DISCUSSIONS

A. Phase diagram without canting and lattice distortion

Figure 1 shows the phase diagram at zero temperature in the plane of the doping concentration (x) and the AF interaction between t_{2g} spins (J_S), without the electron-lattice coupling ($g = 0$). Orbital shape is represented by p- [planar, orbital F (0,0), i.e., $d_{x^2-y^2}$] and n- [nonplanar, orbital G (100,−100) around $x = 0.1$ and orbital A (−40,−40) around $x = 0.7$] hereafter. The possibility of the spin canting is not taken into account, i.e., $\eta = 0$ or π. For $J_S = 0$, spin F is the most stable for almost the whole region of x, except around $x = 0$. This ferromagnetism comes from the superexchange interaction between e_g spins for small x ($x \sim 0.1$), and from the double exchange interaction for larger x ($x \sim 0.7$).[8,30] Nonmonotonic behavior with double peaks ($x = 0.1$, 0.7) of the phase boundary between spin F and A [$J_S(FA)$] is then attributed to the crossover from the super- to the double-exchange interaction, similarly to the case of 113-system.[8] We identify the spin transition from spin F to spin A with increasing x observed experimentally for $0.3 < x_{exp.} < 0.5$ (Refs. 6,16–26) with that around $x \sim 0.15$ when $J_S \lesssim 0.006$ eV [for example, arrow (a) or (b) in Fig. 1]. This value of J_S is roughly of the same order in magnitude as the 113 case.[8,7] Depicted orbital alignment is the one optimized at each point of the phase diagram. For most of the phase diagram, $d_{x^2-y^2}$ is the most stable one reflecting the two-dimensional nature of the double-layered structure. The spin C phase completely disappears. One might regard this as self-evident because of the two-dimensionality. This, however, is not so trivial be-

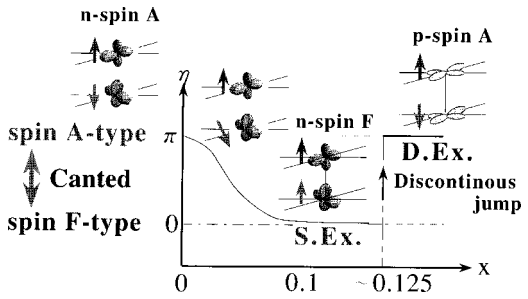

FIG. 2. The x dependence of the optimized canting angle η with $g=0$.

cause the valency along c axis can still lower the energy by the bonding/antibonding splitting for the double-layered structure.

B. Spin canting

We now study the spin canting between spin F and A. First, we consider the possibility of the spin canting with fixed $J_S=0.004$ eV, shown as the arrow (a) in Fig. 1.

The x dependence of the optimized canting angle η is shown in Fig. 2. The electron-lattice coupling is not considered ($g=0$). The canting angle changes continuously from π (spin A, $x=0$) to zero (spin F, $x\sim0.1$), corresponding to the spin canting around the parent insulator. In this region, the orbital alignment almost remains that for $x=0$ [orbital G (100,−100)], implying that the ordering is still dominated by the superexchange interaction in this region. This is consistent with the interpretation that the peak of the phase boundary $J_S(FA)$ around $x=0.1$ is attributed to the superexchange interaction. Coexisting double exchange interaction due to the introduced carriers competes with J_S, leading to the spin canting seen for $0<x<0.1$ in Fig. 2 through the conventional mechanism a la de Gennes[15] for 113 system. Battle *et al.* observed the coexistence of the spin F and A by the powder diffraction of the polycrystal sample $La_2SrMn_2O_7$ ($x=0$).[31] This can be explained by small amount of carriers introduced by the oxygen deficiencies which brings about the spin canting by this mechanism for small x region, as reproduced in Fig. 2. When x goes beyond $x\sim0.125$, η discontinuously changes from zero to π, corresponding to the first-order transition from spin F to spin A. This behavior without canting is due to the discontinuous orbital transition. With increasing the double-exchange interaction for $x>0.1$, the orbital discontinuously changes from orbital G (100,-100) to orbital F (0,0), i.e., $d_{x^2-y^2}$, in order to maximize the kinetic energy gain. With fixed J_S as in Fig. 2, the spin transition between spin F and A is accompanied with this orbital transition (n-spin F to p-spin A). Therefore, the spin canting observed for $0.4<x_{exp.}<0.5$ in the single-crystal samples,[19–22,25,26] therefore, cannot be reproduced in Fig. 2.

In order to explain this experimental observation, we look for the possible mechanisms for the continous change of spin/orbital structure starting from the p-spin A. One possibility is to change the orbital wave function via the coupling to the lattice. In 327 system,[18,22–26] the lattice constant c is longer than a, b, which prefers $d_{3z^2-r^2}$ compared with $d_{x^2-y^2}$, and c changes as x. This corresponds to the ''magnetic field'' to the orbital pseudospin, and tends to enhance the transfer along z direction and hence the spin canting.

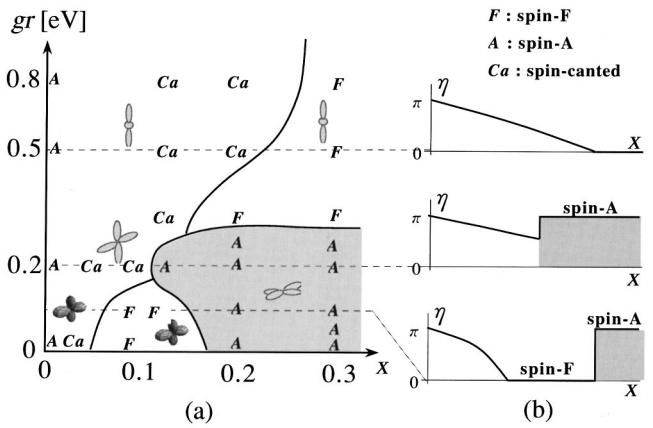

FIG. 3. The phase diagram as a function of the doping concentration x and the electron-lattice coupling g. p-spin A is always surrounded by the discontinuous boundary with respect to η.

In Fig. 3 is shown the phase diagram in the plane of x and gr (g: coupling constant, r: elongation along c axis). This gr corresponds to the ''orbital magnetic field'' to prefer $d_{3z^2-r^2}$. Here, J_S is fixed to be 0.004 eV, which is comparable to the value appropriate for 113 system.[7,8] The p-spin A state [shaded in Fig. 3(a)] is surrounded by the discontinuous ''orbital spin-flop'' transition. This is because the ''orbital magnetic field'' gr is applied not perpendicularly but antiparallel to the $d_{x^2-y^2}$ direction. Therefore, it seems unlikely that the spin canting occurs between the p-spin A and spin F with *different* orbital structures, e.g., the arrow (a) in Fig. 1.

We now look for the possibility of the spin canting with the orbital structure fixed to be $d_{x^2-y^2}$, i.e., the arrow (b) in Fig. 1. The corresponding J_S value might appear to be too small (~0.0002 eV), but J_S is very sensitive to the bond length l ($J_S\sim l^{-14}$ as discussed later), and the lattice elongation along c axis suggests smaller value of J_S in 327 system compared with 113. Furthermore, the x dependence of l induces the x dependence of J_S and the arrow (b) in Fig. 1 has finite vertical component. Another remark is that even though the orbital pseudo-spin $\vec{T}_i$ is fully polarized along $d_{x^2-y^2}$-direction, the wave fuction is the hybridized one with $d_{x^2-y^2}$ and $d_{3z^2-r^2}$. Namely the $d_{3z^2-r^2}$ has the weight $\sim(t_0/\tilde{\beta})^2$, which induces the effective transfer t_z between layers. However, t_z is much smaller than t_0, which is crucial to the spin canting as discussed below.

In Fig. 4 is shown the energy as a function of the angle η between the spins of two layers for several values of J_S. Spin F for $J_S=0$ is due to the above-mentioned double-exchange interaction with the weight $\sim(t_0/\tilde{\beta})^2$. For $J_S=0.42$–0.5 meV, the optimized angle η is the intermediate between $\eta=0$ and $\eta=\pi$, and the canting state is realized. Therefore, we conclude that the spin canting occurs between p-spin A and p-spin F states when J_S changes.

In order to study further this canting state, we introduce a simplified model shown in Fig. 5. We assume that the spin polarization is perfect, i.e., all the electron spins are aligned along the ordered direction. Therefore we consider the spinless fermions. The density of states is taken to be a constant N_F for each layer. We take the hole picture, and x holes are occupying this constant density of states from the bottom. These two bands are split into bonding and anti-bonding

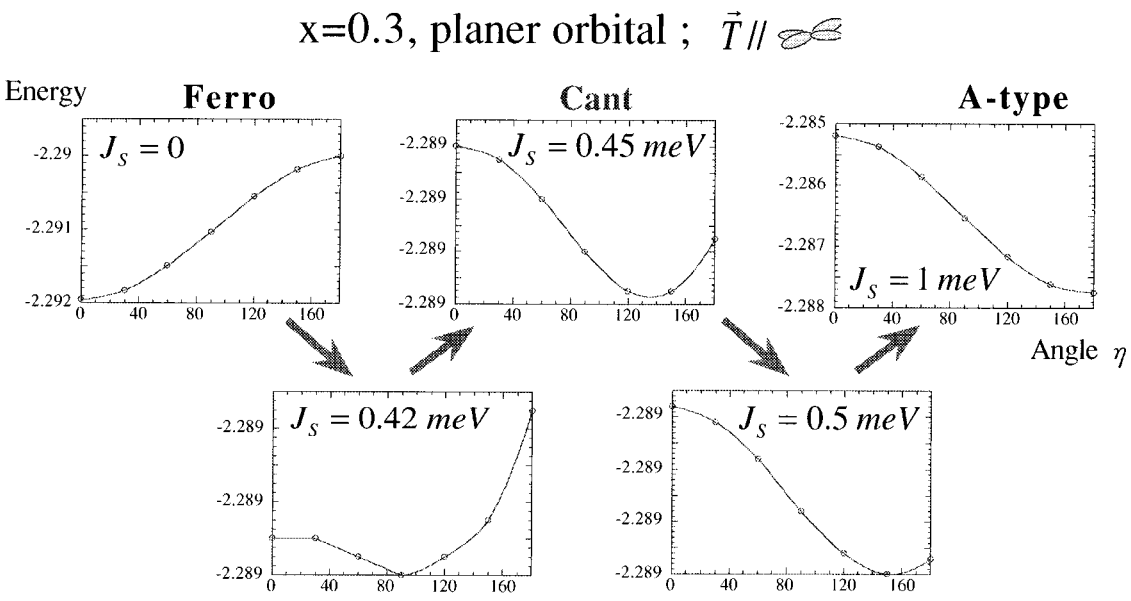

FIG. 4. η dependence of the ground state energy calculated for a planar orbital ($\vec{T}$ points to the direction of $d_{x^2-y^2}$), which saddle point corresponds to the canting angle.

ones with the splitting $\Delta = t_z \cos \eta/2 = t_z \xi$.[32] The kinetic energy gain $\Delta E_{kin}(\xi)$ is given by

$$\Delta E_{kin}(\xi) \sim \begin{cases} -t_z^2 \cdot N_F \cdot \xi^2 & (\text{for } \xi < \xi_c \equiv x/N_F t_z) \\ -t_z \cdot x \cdot \xi & (\text{for } \xi > \xi_c), \end{cases} \tag{7}$$

while the energy cost of the exchange interaction is $J_S \cos\eta = J_S(2\xi^2 - 1)$. The lower line of Eq. (7) is obtained by de Gennes, and if this holds the canting always occurs.[15] The new aspect here is that $\Delta E_{kin}(\xi) \propto \xi^2$ when the splitting $\Delta = t_z \xi$ is smaller than the Fermi energy $\epsilon_F = x/N_F$ and both the bonding and anti-bonding bands are occupied. Therefore, the spin A structure ($\xi = 0$, $\eta = \pi$) is at least locally stable when $2J_S > t_z^2 N_F$. This condition can be satisfied when the orbital is almost $d_{x^2-y^2}$ and t_z is much reduced from t_0. For general orbital configuration $t_z^2 N_F$ is order of magnitude larger than J_S. Now, we look for the optimized ξ to minimize the total energy $\Delta E(\xi) = \Delta E_{kin}(\xi) + \Delta E_{ex}(\xi)$. When $\xi_c > 1$ ($x > t_z N_F$), only the upper line of Eq. (7) is relevant and $\Delta E = (2J_S - t_z^2 N_F) \cdot \xi^2$. Therefore ξ jumps from 1 (spin F) to 0 (spin A) as J_S increases across $t_z^2 N_F/2$.

When $\xi_c < 1$, the optimized ξ as a function of J_S is given in Fig. 6. As J_S increases, the spin structure changes as spin F ($J_S < t_z x/4$) $\rightarrow$ spin canting ($t_z x/4 < J_S < t_z^2 N_F/4$) $\rightarrow$ spin canting with fixed canting angle ($t_z^2 N_F/4 < J_S < t_z^2 N_F/2$) $\rightarrow$ spin A ($t_z^2 N_F/2 < J_S$). Note that the canting angle continuously evolves from spin F, but jumps at the transition to the spin A. Summarizing, $x < t_z N_F$ and $t_z x/4 < J_S < t_z^2 N_F/2$ are the condition for the occurrence of the spin canting. Considering $N_F \sim 1/t_0$, and J_S is about two orders of magnitude smaller than t_0, this condition is satisfied only when t_z is much reduced from t_0 and x is small. Spin canting state does not appear in Fig. 2 because of the large t_z for n-spin F.

Spin canting observed in the metallic region $0.4 < x_{exp.} < 0.5$ (Refs. 19–22,25,26) implies therefore the planar orbital in this region. This is consistent with the spin easy axis observed within the ab plane in this region[20,22,26] because the planar orbital leads to this anisotropy of the easy axis according to the spin Hamiltonian derived by Matsumoto[33] taking into account the spin-orbit interaction. The observed spin

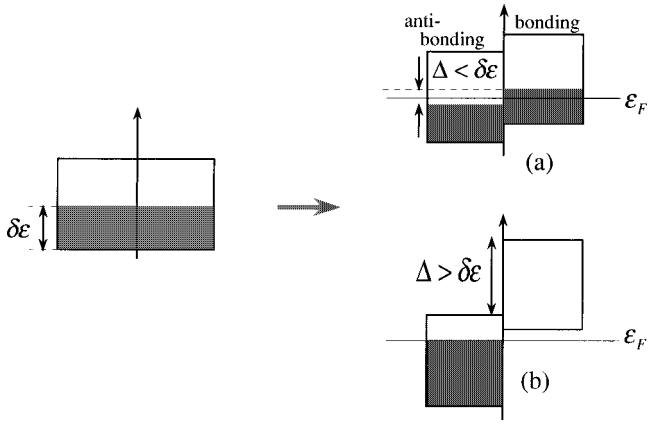

FIG. 5. The bonding/antibonding splitting of the band by the interlayer hopping. The small (large) splitting case is depicted as (a) [(b)].

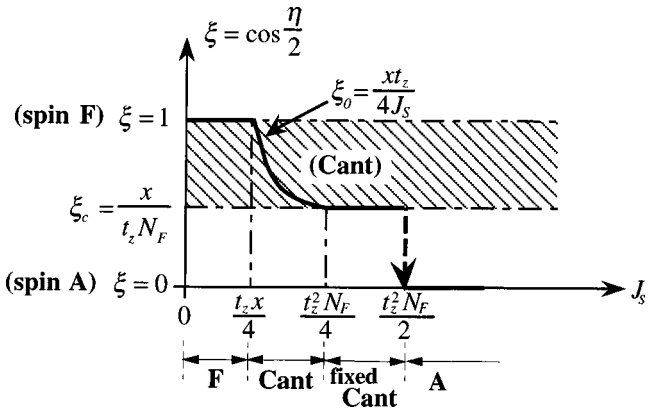

FIG. 6. Canting saddle point ξ as a function of J_S (for the case $\xi_c \leq 1$).

transition from F to A with increasing x should therefore correspond to that from p-spin F to p-spin A in Fig. 1, for which the increase in J_S with increasing x is needed [arrow (b) in Fig. 1].

This x dependence of J_S can be explained in terms of the bond-length dependence of the interlayer hopping integral. According to the pseudo-potential theory,[34] the hopping integral between the d orbitals depends on the bond length l as $t \propto l^{-7}$, leading to $\xi_0 \propto t^z_{e_g}/(t^z_{t_{2g}})^2 \propto l_c^7$, where l_c denotes the bond length along c axis. The observed lattice contraction along c axis with increasing x[23] therefore gives rise to the decrease of ξ_0, leading to the spin structure changes from spin F to cant, and to spin A. $J_S^z \propto (t^z_{t_{2g}})^2 \propto l_c^{-14}$ increases due to this lattice contraction along c axis, which can explain the x dependence of J_S needed for the change from p-spin F to p-spin A, as shown by the arrow (b) in Fig. 1.

The neutron-diffraction experiments have revealed that the samples with the spin canting at zero temperature ($0.4 < x_{exp.} < 0.48$) become the spin A at higher temperatures.[22] This can also be explained in terms of the lattice deformation as follows. The observed lattice contraction along c axis[18,25,22] with increasing temperature brings about the decrease of $\xi_0 \propto t_z/J_S \propto l_c^7$, leading to the spin transition toward the spin A discontinuously. Hirota *et al.* also attributed this T-dependent spin transition to the lattice deformation.[22]

As seen above, the observed lattice deformation plays an important role to explain the spin transition. In our scenario, the bond-length dependence of the inter-layer hopping is the most important mechanism which relates the lattice and the electron systems. One might, however, attribute it rather to the Jahn-Teller type electron-lattice interaction through the electro-static coupling (in other words, the ''orbital magnetic field''). In this scenario, the lattice contraction along c axis reduces the hybridization of $d_{3z^2-r^2}$ orbital as x increases, namely the stabilization of $d_{x^2-y^2}$, which prefers spin A.[22] According to this scenario, the temperature dependence of the spin canting mentioned above is also explained by the change in the hybridization of $d_{3z^2-r^2}$[22] which is brought about by the temperature-dependent lattice elongation. This scenario, however, results in the decrease of the interlayer hopping as x (T) increases, being opposite to our scenario, where little change in the orbital ordering and the increase of the inter-layer hopping $t_z \propto l_c^{-7}$ during the spin transition are predicted. Main distinction between these two scenarios is whether such a large change in the hybridization of $d_{3z^2-r^2}$ occurs during the spin transition or not. As seen in Fig. 2 and Fig. 3, however, the spin transition should be of the first order without canting if it is accompanied with the large change in the orbital. Experimentally, the spin easy axis falls onto ab plane discontinuously around $x_{exp} = 0.32$ (spin F) (Refs. 23 and 26) and the spin transition from F to cant, and to spin A occurs with this easy axis being unchanged. This behavior implies that the hybridization of $d_{3z^2-r^2}$ decreases discontinuously before the spin transition, and during the transition the wave function is almost planar as $d_{x^2-y^2}$, namely the transition is between p-spin F and p-spin A with canting. Though, even in this case, the ''orbital magnetic field'' brings about a little change in the hybridization of $d_{3z^2-r^2}$ via the change of the weight mentioned before,

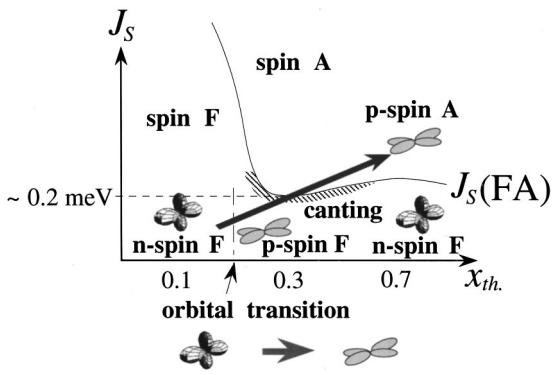

FIG. 7. Schematic sketch of the calculated phase diagram and the correspondence with the experiments.

$(t_0/\tilde{\beta})^2 \rightarrow [t_0/(\tilde{\beta} - gr)]^2$, it is a minor correction comparing with the sensitively changing bond-length dependence, $t^z \propto l_c^{-7}$, $J_S \propto l_c^{-14}$.

For the spin canting, $\xi_0 = t^z x/4J_S < 1$, and hence the planar orbital during the spin transition turned out to be essential. In 113-system, the spin F phase neighboring the metallic spin A has the quasi-three-dimensional orbital ordering for the realistic parameters in the mean field theory.[7,8] Therefore, the canting does not occur because the orbital structures are *different* between spin A and F, and the transition between them is always discontinuous. In the real 113 system no anisotropy has been reported in the spin F state, and there is a theoretical suggestion of the orbital liquid state for the spin F metallic region.[28] In any case the orbital state is different from the $d_{x^2-y^2}$ in the metallic spin A state. In 327 case, the layered crystal structure brings about the two-dimensional orbital anisotropy, reflecting the interplay of the dimensionality of the crystal structure and that of the orbital ordering.

Figure 7 summarizes our interpretation of the experiments (notations $x_{th.}$ and $x_{exp.}$ are used to prevent confusion due to the quantitative discrepancy of x between the calculations and the experiments). The hatched region corresponds to the spin-canting phase due to the planar orbital for the p-spin F. $J_S(FA)$ is the phase boundary with the first-order transition between spin F (or canting) and spin A. Spin F phase at $x_{exp.} = 0.3$ (Ref. 17) corresponds to the n-spin F phase. With increasing x, spin F changes from n- to p- with the orbital transition into $d_{x^2-y^2}$ around $x_{th.} \sim 0.125$. This transition is of the first order, leading to the discontinuous reorientation of the spin easy axis from being along c axis into within the ab plane by considering the spin-orbit interaction.[33] This explains the observed spin anisotropy[20,22,26,27] where the easy axis, pointing parallel to the c axis for $x_{exp.} = 0.3$,[27] discontinuously turns onto the ab plane at $x_{exp.} \sim 0.32$,[26] for $T \lesssim 100$ K. The p-spin F phase around $x_{th.} \gtrsim 0.125$ cants readily within the ab plane because of the decrease in $\xi_0 \propto l_c^7$ due to the contraction of the bond length along c axis with increasing x, and then discontinuously jumps to the p-spin A, corresponding to the observation for $0.4 < x_{exp.} < 0.5$.[19–22,25,26]

In conclusion, we have studied the spin and the orbital ordering in 327 system, taking the orbital degrees of freedom and the strong Coulombic repulsion into account. Observed x

dependence of the spin ordering and its anisotropy were qualitatively explained in terms of the orbital ordering and the observed lattice deformation along *c* axis. The observed temperature dependence of the spin structure is also explained by the lattice deformation. The difference between 327 system with canting and 113 system without canting is understood in terms of the difference in the dimensionality of the crystal strucuture.

ACKNOWLEDGMENTS

The authors would like to thank K. Hirota, Y. Endoh, T. Akimoto, Y. Moritomo, S. Ishihara, W. Koshibae, S. Maekawa, H. Yoshizawa, T. Kimira, and Y. Tokura for their valuable discussions. This work was supported by Priority Areas Grants from the Ministry of Education, Science and Culture of Japan.

[1] K. Chahara, T. Ohono, M. Kasai, Y. Kanke, and Y. Kozono, Appl. Phys. Lett. **62**, 780 (1993).

[2] R. von Helmolt, J. Wecker, B. Holzapfel, L. Schultz, and K. Samwer, Phys. Rev. Lett. **71**, 2331 (1993).

[3] Y. Tokura, A. Urushibara, Y. Moritomo, T. Arima, A. Asamitsu, G. Kido, and N. Furukawa, J. Phys. Soc. Jpn. **63**, 3931 (1994); A. Urushibara, Y. Moritomo, T. Arima, A. Asamitsu, G. Kido, and Y. Tokura, Phys. Rev. B **51**, 14 103 (1995).

[4] S. Jin, T. H. Tiefel, M. McCormack, R. A. Fastnacht, R. Ramesh, and L. H. Chen, Science **264**, 413 (1994).

[5] R.A. Ram, P. Ganguly, and C.N. Rao, J. Solid State Chem. **70**, 82 (1987).

[6] Y. Moritomo, Y. Tomioka, A. Asamitsu, Y. Tokura, and Y. Matsui, Phys. Rev. B **51**, 3297 (1995); Y. Moritomo, A. Asamitsu, H. Kuwahara, and Y. Tokura, Nature (London) **380**, 141 (1996).

[7] R. Maezono, S. Ishihara, and N. Nagaosa, Phys. Rev. B **57**, R21 822 (1998).

[8] R. Maezono, S. Ishihara, and N. Nagaosa, Phys. Rev. B **58**, 11 583 (1998).

[9] H. Kawano, R. Kajimoto, H. Yoshizawa, Y. Tomioka, H. Kuwahara, and Y. Tokura, Phys. Rev. Lett. **78**, 4253 (1997).

[10] Y. Tomioka (unpublished).

[11] H. Kuwahara, T. Okuda, Y. Tomioka, T. Kimura, A. Asamitsu, and Y. Tokura, in *Science and Technology of Magnetic Oxides*, edited by M. Hundley *et al.*, MRS Symposia Proceedings No. 494 (Materials Research Society, Pittsburgh, 1998), p. 83.

[12] R. Kajimoto, H. Yoshizawa, H. Kawano, H. Kuwahara, Y. Tokura, K. Ohoyama, and M. Ohashi, Phys. Rev. B **60**, 9506 (1999).

[13] H. Kuwahara, T. Okuda, Y. Tomioka, A. Asamitsu, and Y. Tokura, Phys. Rev. Lett. **82**, 4316 (1999).

[14] Y. Moritomo, T. Akimoto, A. Nakamura, K. Ohoyama, and M. Ohashi, Phys. Rev. B **58**, 5544 (1998).

[15] P. G. de Gennes, Phys. Rev. **118**, 141 (1960).

[16] P.D. Battle, M.A. Green, N.S. Larskey, J.E. Millburn, P.G. Radaelli, M.J. Rosseinsky, S.P. Sullivan, and J.F. Vente, Phys. Rev. B **54**, 15 967 (1996).

[17] T. Kimura, Y. Tomioka, H. Kuwahara, A. Asamitsu, M. Tamura, and Y. Tokura, Science **274**, 1698 (1996); T. Kimura, A. Asamitsu, Y. Tomioka, and Y. Tokura, Phys. Rev. Lett. **79**, 3720 (1997).

[18] J.F. Mitchell, D.N. Argyriou, J.D. Jorgensen, D.G. Hinks, C.D. Potter, and S.D. Bader, Phys. Rev. B **55**, 63 (1997); in *Solid-State Chemistry of Inorganic Materials*, edited by P.K. Davies *et al.*, MRS Symposia Proceedings No. 453 (Materials Research Society, Pittsburgh, 1997), p. 343.

[19] D.N. Argyriou, J.F. Mitchell, J.B. Goodenough, O. Chmaissem, S. Short, and J.D. Jorgensen, Phys. Rev. Lett. **78**, 1568 (1997).

[20] D.N. Argyriou, J.F. Mitchell, C.D. Potter, S.D. Bader, R. Kleb, and J.D. Jorgensen, Phys. Rev. B **55**, R11 965 (1997).

[21] T.G. Perring, G. Appeli, Y. Moritomo, and Y. Tokura, Phys. Rev. Lett. **78**, 3197 (1997).

[22] K. Hirota, Y. Moritomo, H. Fujioka, M. Kubota, H. Yoshizawa, and Y. Endoh, J. Phys. Soc. Jpn. **67**, 3380 (1998).

[23] Y. Moritomo, Y. Maruyama, T. Akimoto, and A. Nakamura, Phys. Rev. B **56**, R7057 (1997).

[24] Y. Moritomo, Y. Maruyama, T. Akimoto, and A. Nakamura, J. Phys. Soc. Jpn. **67**, 405 (1998).

[25] T. Kimura, Y. Tomioka, A. Asamitsu, and Y. Tokura, Phys. Rev. Lett. **81**, 5920 (1998).

[26] M. Kubota, H. Fujioka, K. Ohoyama, K. Hirota, Y. Moritomo, H. Yoshizawa, and Y. Endoh, cond-mat/9902288 (unpublished).

[27] T.G. Perring, G. Appeli, T. Kimura, Y. Tokura, and M.A. Adams, Phys. Rev. B **58**, R14 693 (1998).

[28] S. Ishihara, M. Yamanaka, and N. Nagaosa, Phys. Rev. B **56**, 686 (1997).

[29] H. Fujioka, M. Kubota, K. Hitota, H. Yoshizawa, Y. Moritomo, and Y. Endoh, J. Phys. Chem. Solids (to be published).

[30] S. Okamoto, S. Ishihara, and S. Maekawa, cond-mat/9909321 (unpublished).

[31] P.D. Battle, D.E. Cox, M.A. Green, J.E. Millburn, L.E. Spring, P.G. Radaelli, M.J. Rosseinsky, and J.F. Vente, Chem. Mater. **9**, 1042 (1997).

[32] P.W. Anderson and H. Hasegawa, Phys. Rev. **100**, 675 (1955).

[33] G. Matsumoto, J. Phys. Soc. Jpn. **29**, 606 (1970).

[34] W. A. Harrison, *Electronic Structure and the Properties of Solids, The Physics of the Chemical Bond* (Freeman, San Francisco, 1980).